

FURTHER DEVELOPMENTS IN SIMPLE TOTAL ENERGY SENSORS

Oran W. Nicks
Langley Research Center

SUMMARY

In 1976, research results were published on a simple total energy probe concept using principles of laminar flow around a cylinder. A number of probes employing these principles have been built. Additional tests have been conducted to further support earlier findings and options for probes made of a single bent-up tube.

Total energy pressure relationships are reviewed and flow fields around cylinders normal to and inclined to the flow are described. A variety of bent-up probe configurations were tested to explore variations in geometry. Test results are presented on the effects of sensor length, hole location, and angle of sweep. Comparisons are made with other probe tests reported in the literature.

A brief summary of damping restrictors and their use in filtering gusts is presented. Flow field effects, indicating the variables involved for different mounting locations on aircraft, are discussed.

INTRODUCTION

Since the 1976 publication of research results on a simple total energy sensor using principles of laminar flow around a cylinder, reference 1, a number of developments in their application have occurred. One objective of the research was to help sailplane owners improve their soaring instrumentation with a simple "do it yourself" design for a total energy sensor, references 2 and 3; the principles and broader applications are outlined in the Patent description, reference 4.

Many sensor probes have been made embodying the principles advanced; some are in use and reported to be performing quite satisfactorily, a number of modifications have been reported to suit the individual application, and some difficulties have been encountered with home-built sensors and applications for various reasons. In order to expand the general reference knowledge of the principles and sensitivities involved, this report provides information and data on further analyses and tests of simple total energy sensors using principles of laminar flow around a cylinder.

TOTAL ENERGY - PRESSURE RELATIONSHIPS

First, it is appropriate to briefly review the physical relationships of gliding flight which make a total energy sensor useful. Figure 1 shows how the useful total energy of a sailplane can be visualized in terms of altitude and velocity. The potential energy is directly proportional to altitude, the kinetic energy is directly proportional to the square of the velocity, and the sum of potential and kinetic energies is the total energy. At a particular instant, the best indications of the total energy state are provided to the pilot by the altimeter and airspeed indicator. For real-time energy management, however, the rate of change in this total energy state is most important. The basic requirement for a total energy sensor is to help provide the pilot such an indication.

When a sailplane dives, it gains kinetic energy at the expense of potential energy; the opposite occurs in a zoom; however, the only change in total energy during such maneuvers is caused by the drag of the sailplane and atmospheric energy variations, if any. The steady state drag effects are proportional to the drag times the velocity squared as indicated by a sailplane "polar" (where "polar" is defined as sink rate vs. airspeed), and the most significant atmospheric effects are rising and sinking air currents. Secondary effects on changes in total energy are caused by drag increases during rapid accelerations such as sharp pullups and tight turns, and horizontal wind gradients or shears can be significant near the ground. However, these are generally ignored as secondary during non-aerobatic flight at soaring altitudes. Thus, in simple terms, the rate of change in useful total energy may be indicated by a simple variometer instrument, if the total energy sensor connected to it provides proper compensation for exchanges in velocity and altitude.

We have said that the total energy TE of a sailplane of mass M gliding at a velocity V and at altitude H is:

$$TE = MgH + 1/2 MV^2$$

The energy per unit mass of the sailplane can be written:

$$\overline{TE} = gH + 1/2 V^2 \quad (1)$$

Differentiating to obtain the rate of change gives:

$$d(\overline{TE}) = gdH + 1/2 d(V^2) \quad (2)$$

Assuming constant altitude, making use of the relation $dP_o = -\rho g dH$, where P_o is the ambient static pressure, and $dq = 1/2 \rho d(V^2)$, where $q = 1/2 \rho V^2$ we have:

$$d(\overline{TE}) = \frac{-dP_o}{\rho} + \frac{1/2 d(V^2)}{\rho} \quad (3)$$

Assuming the total energy of the sailplane remains constant, $d(\overline{TE}) = 0$ and equation (3) becomes:

$$dP_0 - dq = 0 \quad (4)$$

Integration of equation (4) yields the following:

$$P_0 - q = P_s \quad (5)$$

where P_s is the constant of integration.

P_s obviously is a pressure and must be positive, since for $q = 0$, $P_s = P_0$. Changes in the pressure P_s therefore provide an indication of changes in total energy of the sailplane. Putting equation (5) in coefficient form:

$$C_p \equiv \frac{P_s - P_0}{q} = -1 \quad (6)$$

THE FLOW OF AIR AROUND A RIGHT CIRCULAR CYLINDER

As indicated in reference 1, a number of sources pointed to the nearly correct pressure relationship on the downstream side of a right circular two-dimensional cylinder aligned normal to the flow, when the size of the cylinder and flow characteristics produce Reynolds numbers based on diameter from about 5,000 to perhaps 350,000. Within this Reynolds number range, the flows are described as subcritical, well established laminar flows before separation occurs.

Figure 2 shows the nature of the streamlines calculated for the flow around a cylinder in this regime, reference 5. The separated flow region results in relatively constant base pressures over the aft 110° to 160° of the cylinder. This large, relatively constant pressure region is the reason that a sensor made from a cylinder is insensitive to angles of yaw or circumferential hole position accuracy within this region. The separated flow does tend to fluctuate, however, and a high frequency vorticity can be sensed with dynamic instrumentation. Fortunately, these rapid pressure fluctuations can be damped and need not compromise a total energy sensor output for practical application.

A sample plot of a typical pressure distribution, figure 3, is shown to illustrate the nature of the pressure distribution in the Reynolds number range of greatest interest. This plot shows the relative sameness of the pressures on the aft side of the cylinder, corresponding with the separation region downstream in the streamline diagram. Such data provided the inspirations to use a small cylinder as a means of achieving the desired pressure relationships for a total energy sensor.

THE INCLINED THREE-DIMENSIONAL CYLINDER AS A TOTAL ENERGY SENSOR

Reference 1 described experimental studies which included the discovery that pressures on the aft side of a cylinder could be modified near the flat end of a three-dimensional cylinder to the value desired for total energy relationships. Further testing showed that sweeping the cylinder forward into the airstream about 20° , combined with a specific hole location relative to the end of the cylinder, produced the proper pressure relationship with an insensitivity to flow inclinations of at least $\pm 10^{\circ}$. This is more than adequate for use during soaring flight, as pitch variations for sailplanes of less than 6° to 8° are normal.

The combination of insensitivities to sideslip and angle of attack is especially desirable features of the simple probe. In addition, data were provided which indicated that the sensor holes could be of various diameters, saw slots, or multiple orifices as long as the average dimensions with respect to the cylinder end were maintained. Two specific total energy probe configurations were described which had been based on laboratory results and flight tests.

The most scientifically significant findings of reference 1 are summarized below for reference during the discussions to follow:

1. Flow normal to a right circular cylinder at subcritical Reynolds numbers produces pressure coefficients very close to the value needed for useful total energy rate of change indications.
2. For the velocity and altitude operating range of sailplanes, practical cylinder diameters of about 4.76 mm (3/16-inch) to 6.35 mm (1/4-inch) provide Reynolds numbers within a range from about 8,000 to 30,000, where sensor pressure coefficient and drag coefficient remain practically constant.
3. Orifices on the downstream side of a cylinder provide pressures that are relatively insensitive to sideslip angles.
4. Whereas pressures on the downstream side of a two-dimensional cylinder produce coefficients that tend to be too negative, it is possible to obtain predictably biased pressures with three-dimensional flow effects on a practical sensor by locating rearward facing orifices a given distance from the end of the cylinder; furthermore, the variation in pressure coefficient with hole distance from the end of the cylinder tends to be linear in the region of interest for coefficients near $C_p = -1.0$.
5. Pressure coefficients on the aft side of such a cylinder remain relatively constant over a range of forward sweep angles from about 10° to 30° ; thus, a nominal cylinder orientation of 20° forward sweep provides a sensor with $\pm 10^{\circ}$ insensitivity to pitch changes.

BENT-UP PROBES - PURPOSE OF TESTS

The fin mounted probe configuration described in references 1, 2, 3, and 4 was made by joining two straight sections of tubing. Many home-builders have made total energy probes from a single piece of tubing bent to provide the 20° forward swept portion, thus eliminating the two-piece manufacturing difficulties and the chance for leaks at the intersection of the two tubes. It is understood that many of the probes made in this way have been made of 6.35 mm (1/4-inch) steel tubing commonly used for hydraulic brakelines or fuel lines. This size tubing offers the strength and stiffness to support an extension of about 40 cm (15 inches) ahead of the fin leading edge.

Homebuilders who had difficulties with such probes report that pressure coefficients too low in absolute value were achieved, thus causing under-compensation in flight. One of the suspected causes of the low pressure coefficients was the likelihood that the bent-up sections of tubing were not long enough to sustain the two-dimensional flow field below the orifice. Further wind tunnel testing has been conducted on simple bent-up probes to determine the effects of various probe lengths on pressure coefficients and to better define the geometry of suitable probes made in this manner.

WIND TUNNEL TEST SETUP AND PROBE CONFIGURATIONS

The small wind tunnel used for the tests outlined in reference 1 was used for these tests. An atmospheric tunnel with velocities on the order of 20 meters (60 feet) per second, it provided Reynolds numbers based on diameter with the 6.35 mm (1/4-inch) tubing of 8,000 to 10,000.

The probe test setup was made to allow a common set of sensors to be used. This insured that no differences in results were caused by manufacturing differences on the sensors or hole location geometry.

A simple mounting arrangement allowed changes in the probe angle of attack so that sensitivity to sweep angle or angle of incidence could be determined. The angle of attack could be varied over a range of 35°. Since the probe had been designed with a forward sweep angle of 20° as the nominal mounting position, this meant that the probes were tested with forward sweep into the airstream over a range of +5° to +40°; for simplicity, all data are presented on that basis. The mounting and angle of attack changing system allowed the sensor to remain in the core of the wind tunnel flow where flow was uniform and velocities constant. As each probe configuration change was made, leak tests were performed to insure sealed joints.

Three types of configurations were tested with a combination of four sensors and two extenders, giving a total series of 13 configurations. These allowed a range of geometric parameters to be tested including sensor length, hole position from the probe end, hole position circumferentially, and two holes at a fixed orientation. These are shown in figure 4.

WIND TUNNEL RESULTS

As indicated in figure 5, variations in the length of the straight section of the sensor above the bend did have an effect on the pressure coefficient for sensors with the end geometry described in reference 1. Sensor lengths of 7 and 9 diameters produced pressure coefficients lower than the desired $C_p = -1.0$, whereas Y/D 's of 11 and 13 both produced $C_p = -1.0$. These data support the findings from earlier tests where Y/D 's of 12 or greater gave satisfactory results. Since the drop-off in coefficient apparently began to occur for lengths between 9 and 11 diameters, sensor lengths of 11 diameters or greater from the bend appear necessary to insure the proper flow effects at an orifice located two diameters from the probe end.

These data also confirm that a nominal forward sweep angle of 20° is a good choice to allow variations in flow direction which may result from downwash, slight mounting misalignments, or attitude changes during flight, without effects on the sensor pressure.

After it was determined that lengths shorter than 11 diameters did not produce the desired pressure coefficient with the hole at $X/D = 2.0$, an experiment was performed to determine whether locating the sensor hole nearer the end of the probe might counteract this effect by capitalizing on the varying effects of hole position discovered earlier. Using bent-up probe configurations having a fixed length/diameter ratio of $Y/D = 7$, results were obtained with three hole positions as indicated in figure 6. These data show that a $C_p = -1.0$ should be achievable for a hole position between 1.5 and 1.75 diameters from the sensor end; however, it is also seen that the range of insensitivity to sweep has lessened somewhat when compared to probes with a hole location 2.0 diameters from the end.

In a personal communication, Frank Irving of Imperial College referred to data on pressure distributions around cylinders normal to the flow showing less variation in pressure coefficient at circumferential hole locations other than 180° . He reported that he had tested probes with two holes located at $\theta = \pm 130^\circ$ which gave good results.

His comments led to a review of earlier data from references 1, 6 and 7 for cylinders normal to the flow. A slight trend toward greater dispersion of coefficient at $\theta = 180^\circ$ as a function of Reynolds number was evident, but perhaps more interesting are trends from reference 8 shown in figure 7 for two-dimensional cylinders swept at various angles to the flow. The trend toward more negative pressure coefficients at higher θ values is seen, along with the interesting fact that differences in coefficient for various sweep angles are less at lower θ values. This led to the conclusion that a broader range of insensitivity to incidence changes might be achieved if circumferential hole positions less than $\theta = 180^\circ$ were used.

Figure 7 shows the variations in pressure coefficient with sweep to be very slight at $\theta = 140^\circ$; for symmetry in a probe, it would be desirable to have two holes at a $\pm\theta$ value. Since it is much easier to position two holes 90° apart at $\theta = \pm 135^\circ$, this was chosen as a practical compromise to keep the two-hole probe as simple as possible to construct.

Tests with the 135° azimuth hole position were conducted using the same probe sensor sections tested earlier with the holes reoriented to $\theta = 135^\circ$, thus insuring consistent and comparable results with the same sensor sections that had been tested at $\theta = 180^\circ$. The tests were conducted at various X/D's for only two Y/D values of 7 and 11. These two probe sensor lengths were used because the results from earlier tests, shown in figures 5 and 6, indicated that coefficients of the desired values could be achieved for these lengths.

The data from tests of the shortest bent-up probe, Y/D = 7 configuration, are shown in figure 8. As indicated, the holes at the $\theta = 135^\circ$ position do increase the range of insensitivity to forward sweep over the range of interest. These data show the best X/D to be 1.75, producing a coefficient $C_p = -1.0$ over a 20° range of sweep angles. However, the mid-range appears biased such that 25° of forward sweep might be better than 20° as a nominal.

In figure 9, similar data are shown for the sensor length, Y/D = 11, found earlier to give consistent results with previous tests of probes employing the same and greater lengths. By comparing these data with figure 5, it is seen that the configuration with the $\theta = 135^\circ$ hole position gave results very comparable to the $\theta = 180^\circ$ hole position, except for the slightly lesser sensitivity to forward sweep.

Finally, as a confirmation check of an actual two-hole configuration, a new two-hole probe was made for Y/D = 7.0, X/D = 1.5, $\theta = \pm 135^\circ$. The results of this test showed consistent results with the single hole tests for $\theta = 135^\circ$ as shown in figure 10. This was expected since no variation in yaw occurred during tests of the single hole probe, but it provided positive assurance. The insensitivity to sweep was significantly extended for the short probe having two holes, although the particular hole location, X/D = 1.50, resulted in slightly over-compensating coefficients. However, as indicated in figure 8, the desired coefficient should be obtainable by locating two holes at X/D = 1.75. Thus, it has been shown that for a short sensor section with a straight length of 7 diameters, a two-hole configuration will produce good compensation. In general, it has been found that the closer the hole is to the end of the probe, the more sensitive the end effects and more rapid changes in coefficients are likely to occur for small variations in the bevel or chamfer. This tends to make tolerances more important; for this reason, it appears that more consistent results can be expected if bent-up probes are made with sensor lengths of 11 diameters or greater with hole positions 2 diameters from the end.

Perhaps a further word should be said about the shape of the end of the sensor and its effects. References 1, 2, 3, and 4 pointed out that the three-dimensional effects of the probe end were affected by the amount of rounding or chamfer of the end. To obtain consistent results, a squared-off end with a very slight chamfer to "break" the sharp edge was recommended. In reference 9, Wells discussed the matter of beveling edges and described a method of making a chamfering tool for this purpose. He indicated values of about 0.066-0.018 mm (0.004-0.007 inch) are typical. Such precision in chamfering has not been found essential, but experience has shown that rounding off the edges too much tends to produce over-compensation, and care is recommended in beveling the edge. While it is difficult to specify and measure dimensions for the beveled edge, it is believed that chamfered surfaces of about 0.013 mm (0.005-inch) are suitable.

COMPARISON OF VARIOUS CONFIGURATIONS

In addition to a number of informal reports of experiences with total energy probes based on the principles outlined in reference 1, several results have been presented in periodicals which are worthy of mention. In reference 9, Wells discussed a method used for calibrating total energy probes and some results of tests. Performance data were not shown; however, the article indicated satisfactory results with a bent tube approach, although the benefits of forward sweep were questioned. The importance of care in beveling the edge was specifically discussed.

Diplom-Physiker Westerboer (ref. 10) described probes made and tested in West Germany of both fin and fuselage mounted types. He indicated that good compensation was achieved and also mentioned other results obtained in Europe. He specifically mentioned that an experimenter from the Braunschweig Akaflieg had also found 60° to 80° forward sweep (equivalent of 10° to 30° measured from vertical) to be optimum. Dimensions given for a bent-up tube version included a straight section for the sensor portion of about 10 diameters. The test results reported in figure 5 show that greater than 9 diameters are required to achieve the desired sensor pressure coefficient; thus, it would seem that Diplom-Physiker Westerboer also confirmed the suitability of this geometry for a bent-up probe configuration.

An article (ref. 11) by Charles W. Shaw described a probe made for a nose mounting installation. The report stated that excellent compensation was achieved, along with improved response rate, and no effects due to sideslip. The probe was mounted on the nose cap of the fuselage and projected eleven inches above the surface at about the 20° forward sweep angle.

A probe using these principles was discussed in reference 12 by Frank Irving. Although a complete description did not accompany the data presented in the article, a photograph of a probe mounted on a sailplane fin indicated it to be a bent tube design. In the description, it was

stated that the design incorporated the 70° bend inclination to the airstream (20° forward sweep); the same as suggested in reference 1. The data show the probe as being relatively insensitive to incidence or angle of attack changes, although variations of 4 percent were indicated at about $\pm 10^\circ$ of incidence.

In the same article, data were presented for a so-called "Modified Nicks" probe which undercompensated; however, no details of the modification were given, so it is not possible to assess the reasons for the undercompensating pressure coefficients. Data from this report on the best probe tested by Irving are shown in figure 11 for comparison with the configurations reported in reference 1 and the bent-up probes reported here. In a personal communication, Irving described his probe as a bent probe configuration having two holes at $\theta = \pm 130^\circ$ at an X/D value of 1.5, with a Y/D of about 7. Based on these data, it appears that the probe tested by Irving has a greater variation during pitch changes than the bent probe versions having sensor lengths of 11 diameters or more as tested and discussed in this report.

As a matter of general interest, it should be mentioned that probes made like configuration A of reference 1 have been tested in the NASA 8-foot Transonic Pressure Tunnel over a Mach number range from $M = 0.15$ to $M = 0.75$. Although test results have not been published, a variety of X/D values were tested confirming the $X/D = 2$ as most suitable for obtaining C_p values of -1.0. The preliminary data show coefficients within 5 percent of the desired value up to $M = 0.3$, with only slightly more variation to $M = 0.75$. The probes are being installed on a transport aircraft for experiments in wind shear detection and total energy management.

DAMPING RESTRICTORS

The separated flow region behind a cylinder operating at subcritical Reynolds numbers produces a fluctuating pressure which may couple with the dynamic characteristics of a sensitive variometer and cause needle oscillations or "vibrata" effects on an audio signal. Enlarging the orifice diameter or changing the tubing volume connecting the sensor to the variometer can affect these natural frequencies without modifying the average signal pressure, but a recommended solution to this effect involves the use of a damping restrictor-volume combination. Even if the natural frequencies of the sensor-variometer system do not cause oscillations, gustiness will produce fluctuations which tend to compromise the usefulness of total energy readings.

The simplest form of damping or gust filter can be made with a simple capillary restrictor and volume placed in the line between the total energy sensor and the variometer. Most mechanical variometers have time constants of about 2-7 seconds, although some electric variometers and a few mechanical models are capable of response times of less than a second (ref. 13). It is doubtful that response times of much less than two seconds are useful when gusty conditions exist; however, a gust filter will become the limiting factor if it has a slower response than the instrument, and the selection of a filter response rate must take this into account (ref. 14).

A good discussion of gust filters and ways to make them appeared in reference 15. The time constant for a restrictor-capacitor pneumatic gust filter is given by the equation:

$$T = (1.06 \times 10^{-7}) \frac{CL}{PD^4} \quad (7)$$

where:

T = gust filter time constant, sec

C = capacity of the gust filter flask, cubic inches

L = length of capillary tube restrictor, inches

P = absolute pressure of the atmosphere at expected flight levels, pounds per square inch

D = internal diameter of capillary restrictor, inches

Theoretically, it is desirable that the filter capacity volume be larger than the variometer flask when the variometer system uses such; however, a capacity equal that of the vario capacity seems to suffice. For electric varios having a built-in volume, a small capacitor may be suitable. For example, good results have been achieved with a fin mounted sensor having a built-in restrictor made of 0.508 mm (0.020 inch) inside diameter capillary 25.4 mm (1 inch) long, when used with an electric vario having a small internal volume. In this case, the length of tubing from the fin to the vario served as a capacitor.

Using the equation above, restrictor lengths have been calculated and presented in figure 12 for two restrictor inside diameters as a function of capacitor volume, for time constants of 1.0 and 2.0 seconds, at an altitude of 1524 meters (5000 feet). From these relationships, it can be seen that restrictors made of 0.508 mm (0.020 in.) or 0.794 mm (1/32-in.) inside diameter tubing are of practical lengths for a total energy system. Gust filtering is very important, and every total energy probe of the types described herein should have a restrictor added into the probe or installed in the line nearby. For fast response varios,

about 2.5 cm (1 inch) of 0.508 mm (0.020 inch), or about 8 cm (3 inch) of 0.794 mm (1/32-inch) tubing should be helpful for gust filtering without introducing undesirable delays, even if the capacitor volume is small.

FLOW FIELD EFFECTS ON TOTAL ENERGY SENSORS

Obtaining the pressure coefficient for good compensation is best achieved if the sensor can be located in the freestream, unaffected by attitude changes of the aircraft. It is not necessary that the local pressure be the same absolute value as the freestream; it is only necessary that the static pressure, relative to freestream, not vary as the aircraft attitude changes. Because of this, a desirable sensor location must take into consideration local flow field changes during maneuvers. There are several aspects of flow fields which may be important:

1. Boundary layer growth along the body
2. Flow angularities caused by the windshield and the wing body intersection
3. Downwash caused by lifting surfaces deflecting the flow
4. Movable control surfaces which may propagate pressure influences upstream
5. Induced velocities above wing or fuselage

The boundary layer consideration is largely relevant if probes are located on the aft portion of the fuselage. Flows tend to parallel fuselage surfaces aft of the wing, so that a location roughly mid-way between the wing trailing edge and the tail offers relatively constant flow conditions for total energy sensors, provided that the sensor is located far enough from the body to avoid the boundary layer at all angles of attack or yaw. For aft fuselage mounting on the upper side, the sensor element should be located about 7 inches above the surface to insure avoidance of boundary layer fluctuations as attitude changes.

Sensors have been located successfully on the noses of sailplanes; however, for this location there often are significant flow angularities as the flow streamlines are diverted around the body. Canopy bumps may cause local effects which would be undesirable, for example, and when positioning at the proper sweep angle, it should be recognized that streamlines parallel the surface at the surface.

High performance sailplanes usually achieve some laminar flow on the nose portion of the fuselage; a performance penalty may result with a probe in the laminar region which triggers an early transition from laminar to turbulent flow. This is not a problem for training sailplanes or others which do not depend on laminar flow for performance. Judgement must be

used in determining the proper sensor sweep angle on a curving surface, and experimenting with flight tests may be necessary.

The vertical fin location usually offers near freestream conditions, provided the probe is positioned so that the fin, rudder, stabilizer and elevator (especially for Tee Tail configurations) are taken into account.

The principal downwash in the flow field at the fin location is caused by the wing deflecting the air to produce lift. A series of calculations have been made to cover the range of effects for typical sailplanes during cruise and climb conditions. The downwash flow angle is a function of the lift coefficient being achieved at a given time. Reference 16 provides a thorough discussion of the mechanisms affecting the downwash as well as analytical methods for use in calculations. Based on these techniques, and the dimensions for short coupled sailplanes like the 1-26, the downwash angle at the fin tip in degrees is about three times the lift coefficient, C_L . In the cruise condition, the lift coefficient for the 1-26 is about 0.5, making the downwash angle only 1.5 degrees. In the climb condition, the lift coefficient is about 1, making the downwash about 3° . For high performance sailplanes having longer wings and fuselages, the downwash values decrease to about half those for a 1-26; that is, the range of downwash angles at the fin may be about 1.2 to 1.8 times C_L degrees. The range of lift coefficients may be somewhat greater due to flaps; however, the total downwash variation for high performance sailplanes may still be less than 3° .

For a fin installation, the sensor should be positioned at least 5 to 10 times the maximum fin thickness ahead of the leading edge (ref. 17). Severe rudder deflections may cause significant lateral flow inclinations; however, the insensitivities of the simple probes described herein are a real advantage. Horizontal tail movements affect the downwash flow field to some extent. When attitude changes are being made, transients may be noticed; however, the effects can be minimized by smooth movements of the control surfaces. Sailplanes that are well balanced will not have very large tail lift coefficients, and therefore small downwash effects.

In summary, a sensor location insensitive to changes in attitude is necessary for operation over a broad range of locations. Aft fuselage and vertical fin locations can be suitable for the probes discussed. Nose installations may be acceptable for low performance sailplanes; however, they must be positioned carefully.

CONCLUDING REMARKS

Experimental pressure coefficients suitable for total energy compensation have been obtained using principles of laminar flow around a small inclined cylinder. To obtain the correct flow relationships, the sensor orifice should be located carefully with respect to the end of a 3-dimensional cylinder; several options for providing the proper relationships have been extended by the current study of probes made of bent-up tubing. Total energy-pressure relationships have been reviewed to explain the principles involved and further explanations of 3-dimensional effects have been presented.

In general, it has been shown that probe sensors with lengths as short as 7 times the outside diameter of the tubing used can be made to work with certain orifice locations. On the other hand, data have shown that sensitivities to manufacturing tolerance and flow incidence angles are reduced when sensor lengths of 11 diameters or greater are used.

Comparative results from a number of experimenters have verified the principles and findings previously presented. The most significant of these probe dimensions are the sensor hole location geometry and the best angle of sweep for compensation that is insensitive to range of angles of incidence.

Damping restrictors are useful to filter gusts and may be simply made by installing a small section of capillary tubing in or near the total energy probe, in series with an appropriate capacitor volume.

Flow field effects around aircraft can affect the compensation of total energy sensors and must be considered. Among the effects are the boundary layer growth, flow angularities, downwash caused by lifting surfaces and movable control surfaces which may propagate pressure influences. The significance of these effects and ways of accounting for them are discussed.

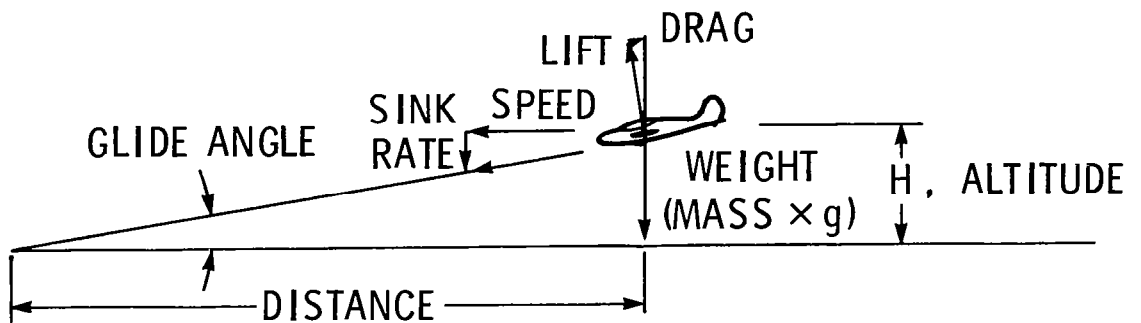


REFERENCES

1. Nicks, Oran W.: A Simple Total Energy Sensor. NASA TMX-73928, March 1976. (Also presented at XV Congress of OSTIV, Ryskala, Finland, June 1976.)
2. Nicks, Oran W.: A Simple Total Energy Sensor. Soaring, Volume 40, No. 9, Sept. 1976.
3. Nicks, Oran W.: How to Make a Total Energy Sensor. Soaring, Vol. 41, No. 3, March 1977.
4. U. S. Patent Office, U. S. Patent No. 4,061,028. Aircraft Total Energy Sensor - Oran W. Nicks, Dec. 6, 1977.
5. Thom, A.: The Flow Past Circular Cylinders at Low Speeds. Proceedings of the Royal Society of London, Series A., Vol. CXLI. Printed for the Royal Society and sold by Harrison and Sons, Ltd., St. Martins Lane, Sept. 1933.
6. Thom, A.: An Investigation of Fluid Flow in Two Dimensions. Reports and Memoranda No. 1194 (AE356). Printed and Published by His Majesty's Stationary Office, London, Nov. 1928.
7. Goldstein, S.: Modern Developments in Fluid Dynamics. Vol. I, Oxford at the Clarendon Press, 1938.
8. Bursnall, William J., and Loftin, Laurence K., Jr.: Experimental Investigation of the Pressure Distribution About a Yawed Circular Cylinder in the Critical Reynolds Number Range. NACA TN 2463, Sept. 1951.
9. Wells, Bill: Calibrating Total Energy Tubes. Soaring, Vol. 41, No. 11, Nov. 1977.
10. Westerboer, Ingo: Die Neue Nicks-Duse: Ein ganz heiber Tip von der OSTIV-Tagung in Finnland. aerokurier, Vol. 9, Sept. 1976.
11. Shaw, Charles: T. E. Sensor, 1-26 Association Newsletter, Jan. 1977.
12. Irving, Frank: A New Total Energy Head. Sailplane and Gliding, Feb.-March 1978.
13. Johnson, Dick: Variometer Time Constants - Soaring Mail - Soaring Vol. 41, No. 6, June 1977.
14. Foster, K., and Parker, G. A.: Fluidics Components and Circuits. Wiley Interscience, A Division of John Wiley and Sons, Ltd., London, New York, Sydney, Toronto.

15. Newgard, Peter M.: Gusts and Gust Filters. Soaring, Vol. 43, No. 1, Jan. 1979.
16. Glauert, H.: The Elements of Aerofoil and Airscience Theory. Second Edition, Cambridge University Press, 1948.
17. Gracey, William: Measurement of Static Pressure on Aircraft. NACA Report 1364, 1958.

PHYSICAL RELATIONSHIPS GLIDING FLIGHT



$$\frac{\text{LIFT}}{\text{DRAG}} = \frac{\text{DISTANCE}}{\text{ALTITUDE LOSS}} = \frac{\text{SPEED}}{\text{SINK RATE}}$$

POTENTIAL ENERGY ,

$$\text{PE} = \text{HMg} ; \text{ALTITUDE} \times \text{MASS} \times \text{g}$$

KINETIC ENERGY ,

$$\text{KE} = \frac{\text{MV}^2}{2} ; \text{MASS} \times \frac{(\text{VELOCITY})^2}{2}$$

TOTAL ENERGY ,

$$\text{TE} = \text{PE} + \text{KE} = \text{HMg} + \frac{\text{MV}^2}{2}$$

FIGURE 1

CALCULATED STREAMLINES PAST A CIRCULAR CYLINDER

(REF. 5)

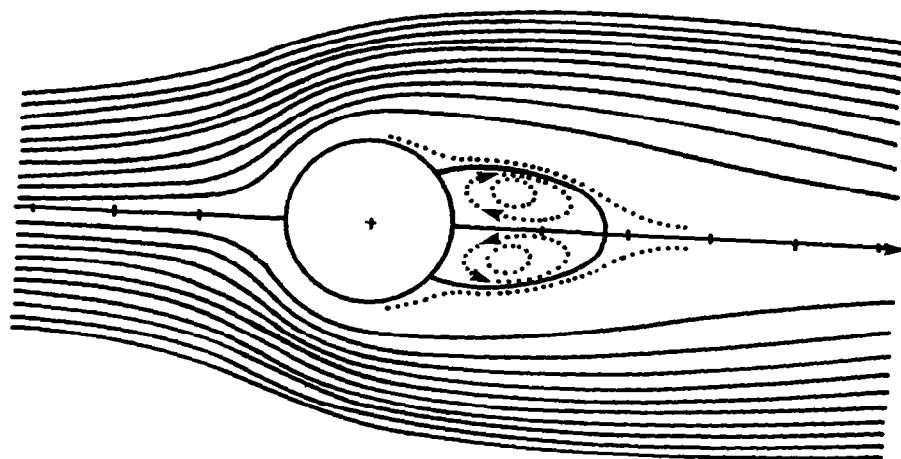


FIGURE 2

TYPICAL PRESSURE DISTRIBUTIONS
TWO-DIMENSIONAL CYLINDERS
 (REFS. 6 AND 7)

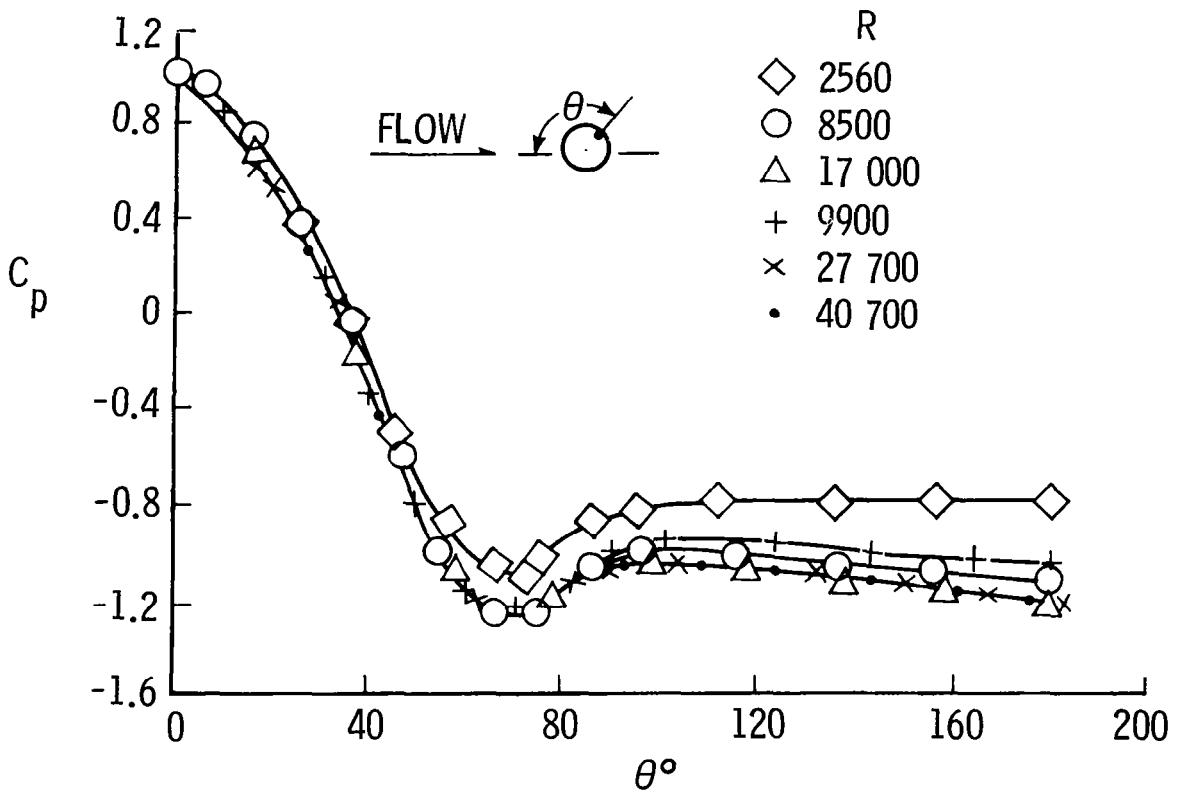


FIGURE 3

BENT-UP PROBE CONFIGURATIONS

CONFIG. NO.	1	2	3	4	5	6	7	8	9	10	11	12	13
Y/D	7	9	11	13	7	7	7	7	7	11	11	11	7
X/D	2.0	2.0	2.0	2.0	1.5	1.75	1.5	1.75	2.0	1.5	1.75	2.0	1.5
HOLE POSITION	$\theta = 180^\circ$												$\theta = 135^\circ$
													$\theta = \pm 135^\circ$

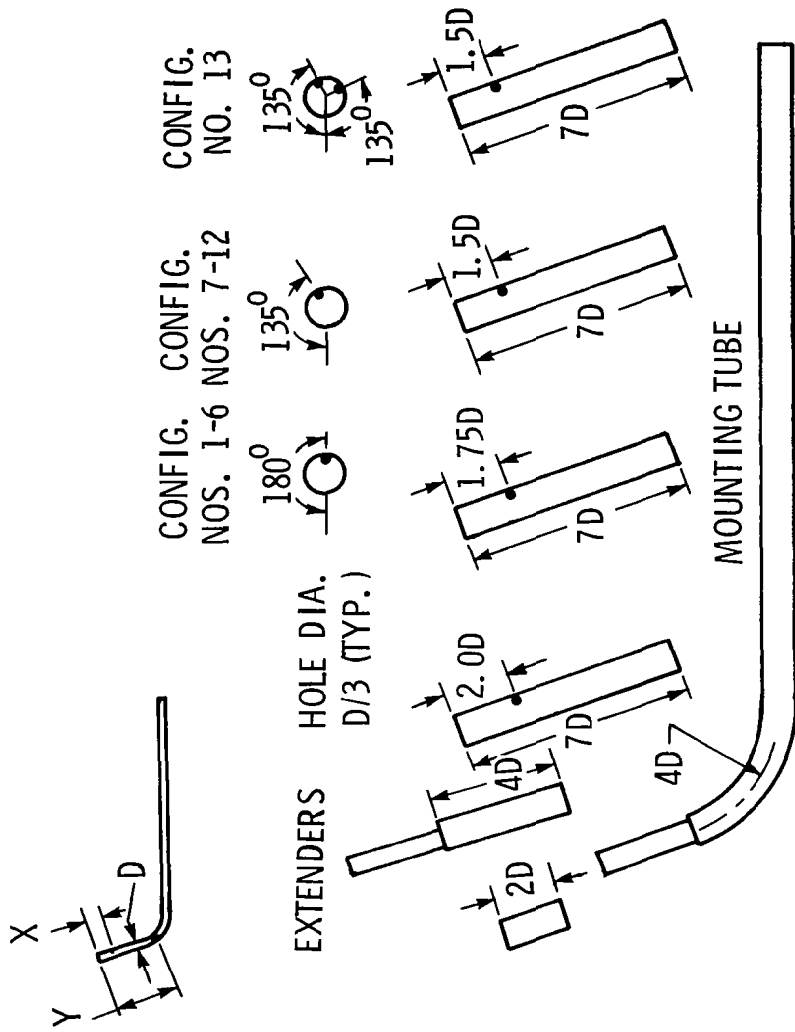


FIGURE 4

EFFECT OF PROBE LENGTH BENT-UP PROBE, $X/D = 2.0$

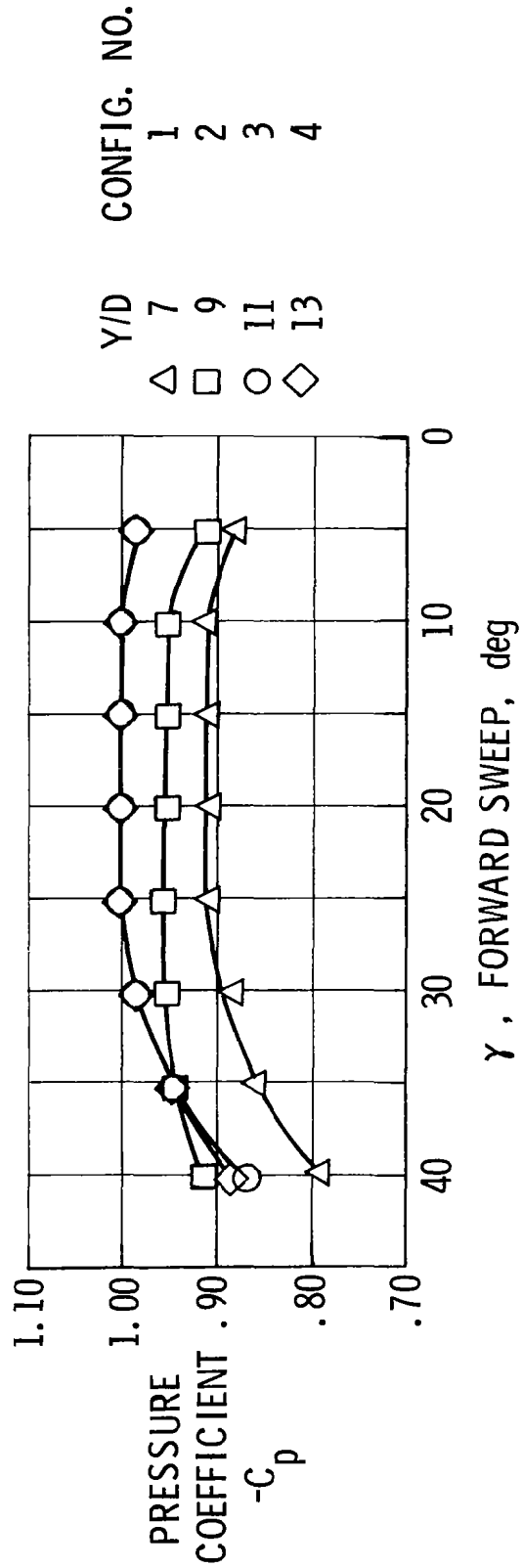
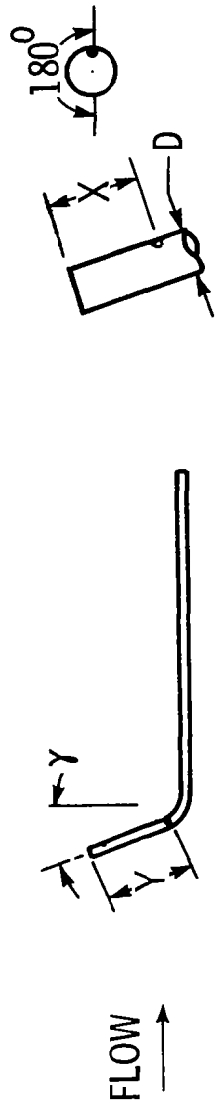


FIGURE 5

EFFECT OF HOLE POSITION SHORT BENT PROBE, $Y/D = 7$

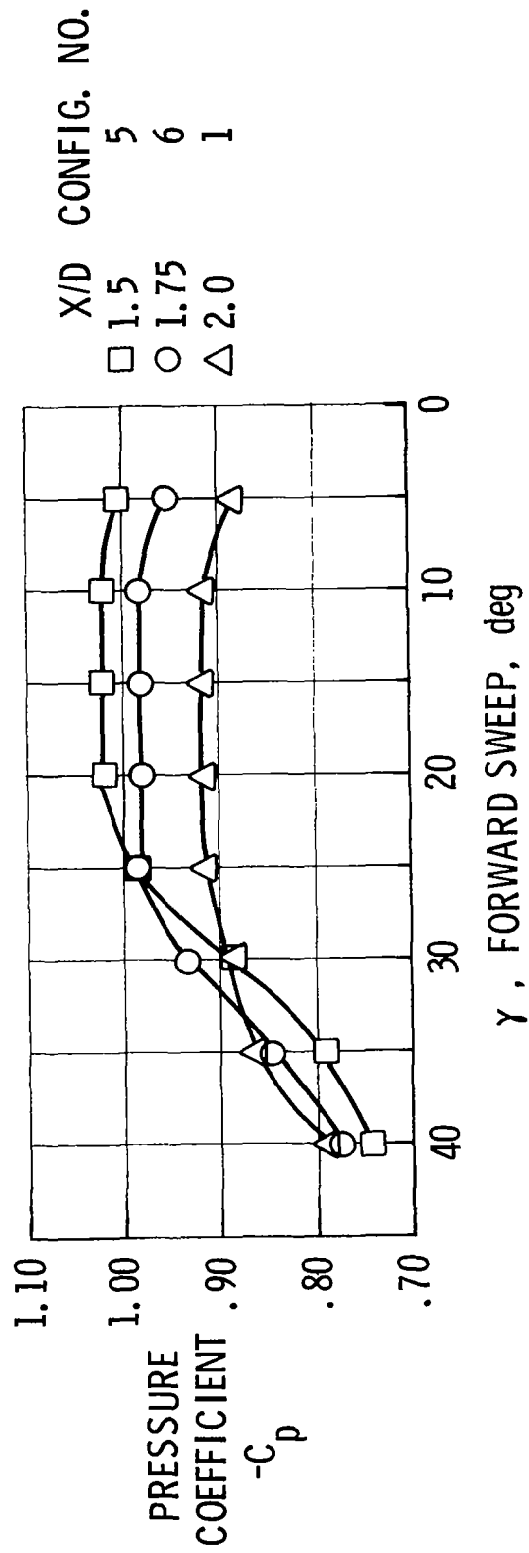
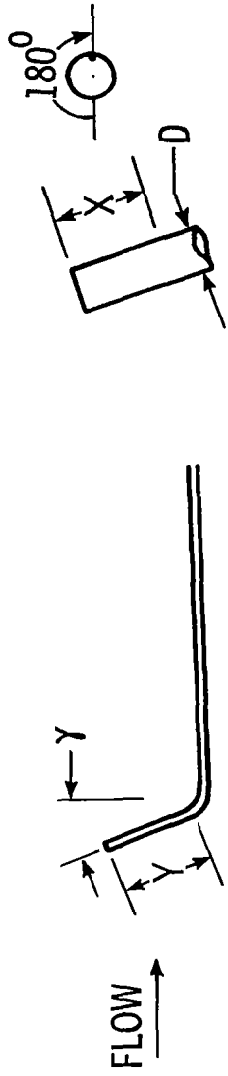


FIGURE 6

PRESSURE DISTRIBUTIONS AROUND A TWO-DIMENSIONAL CYLINDER AT VARIOUS SWEEP ANGLES

(REF. 8)

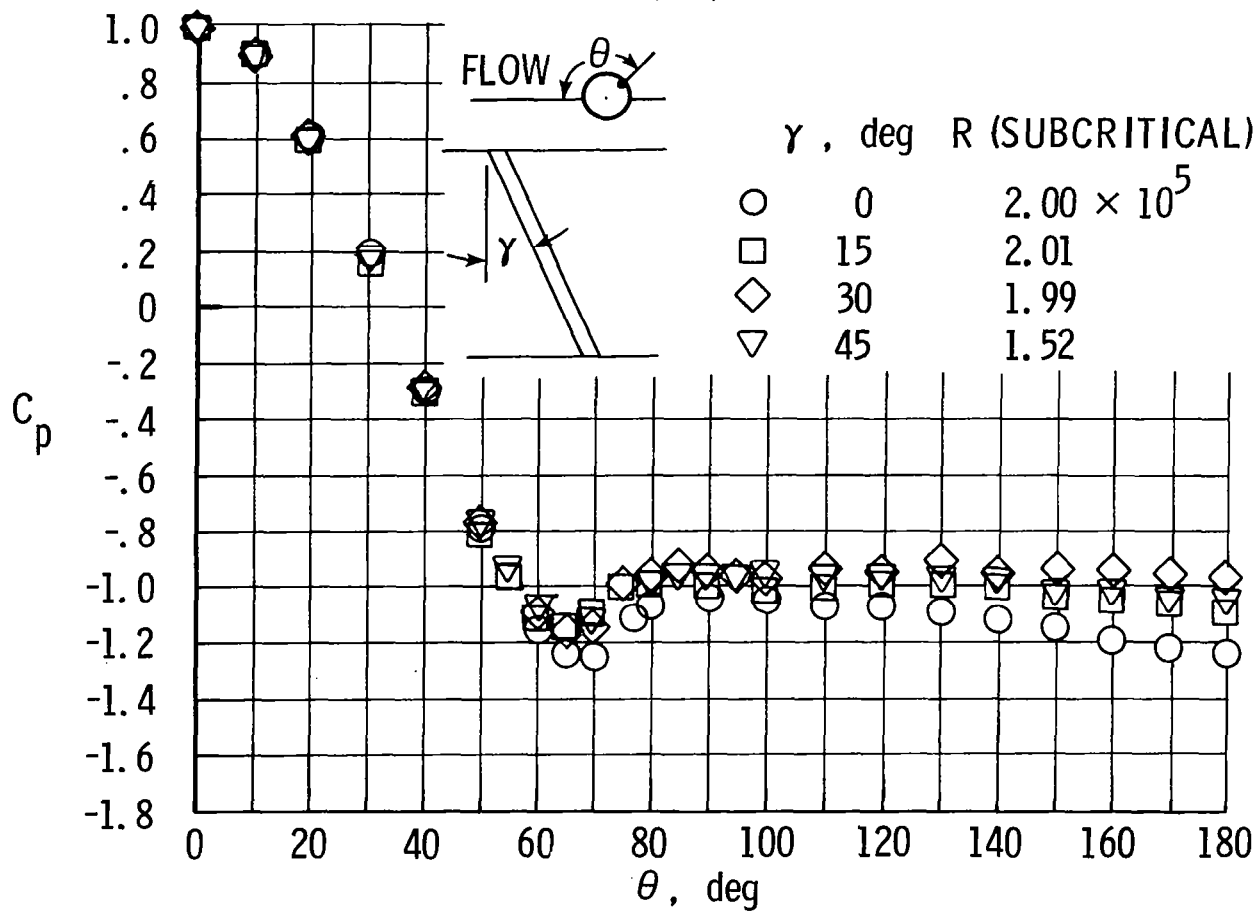


FIGURE 7

**POSITION EFFECT OF ONE HOLE
LOCATED AT $\theta = 135^\circ$; $Y/D = 7$
BENT-UP PROBE**

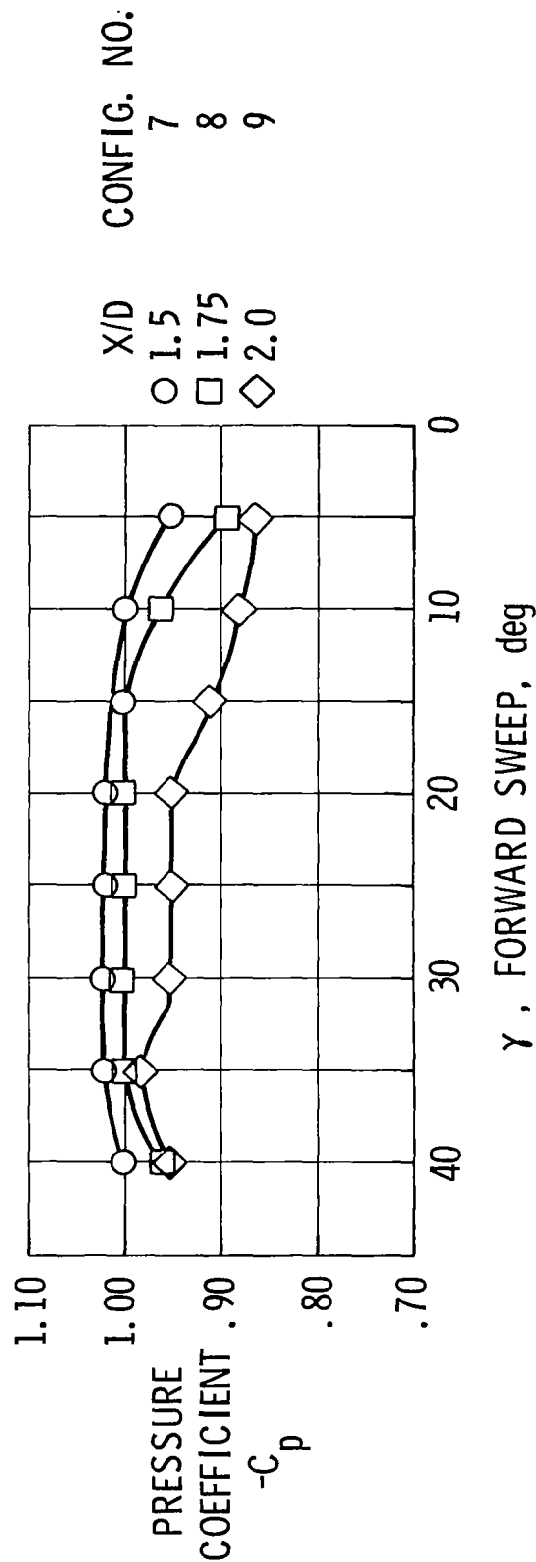
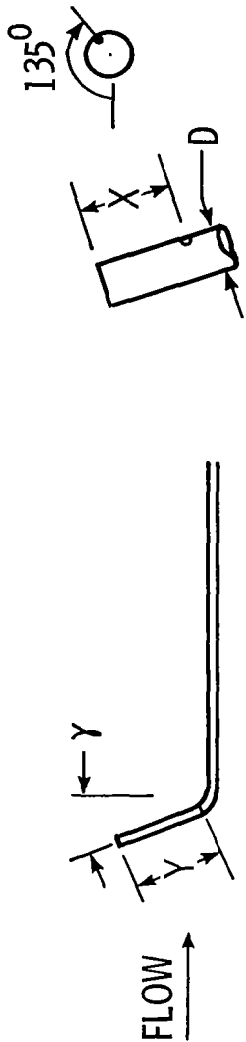


FIGURE 8

**POSITION EFFECT OF ONE HOLE
LOCATED AT $\theta = 135^\circ$, $Y/D = 11$**

BENT-UP PROBE

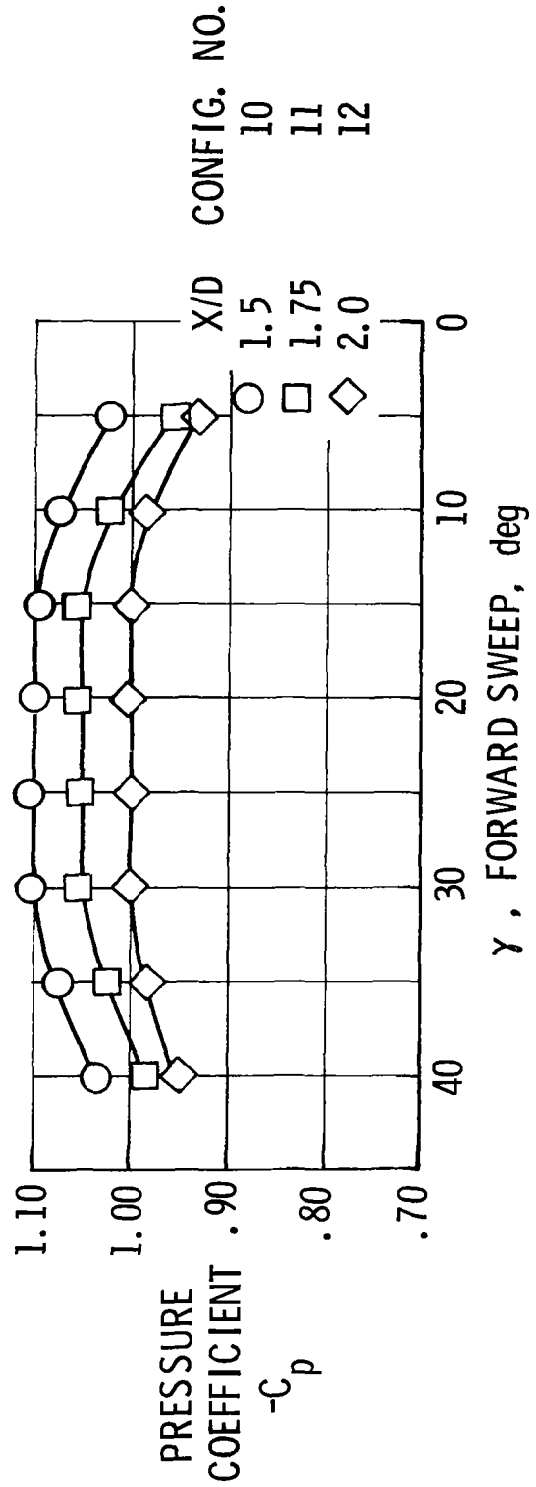


FIGURE 9

**COMPARISON OF ONE HOLE VERSUS TWO HOLES,
 $\theta = 135^\circ$ $Y/D = 7$, $X/D = 1.5$**

BENT-UP PROBE

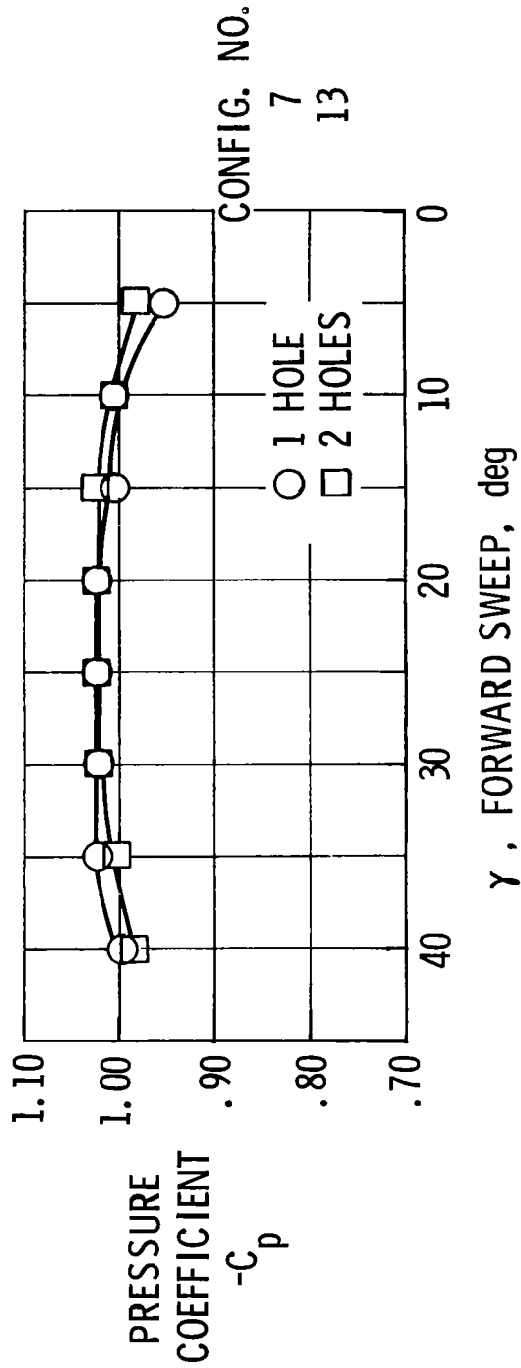
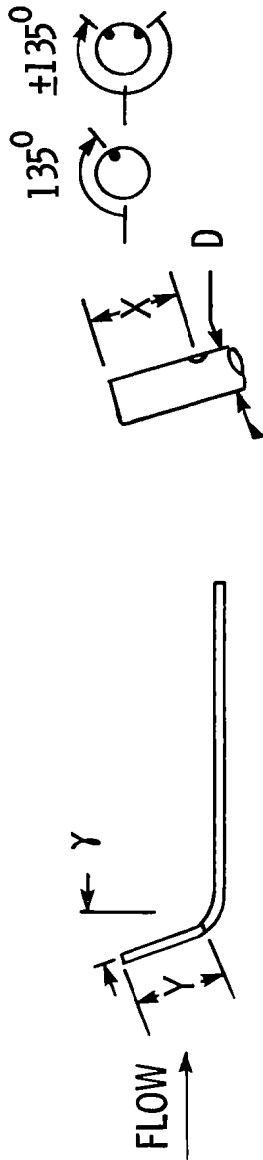
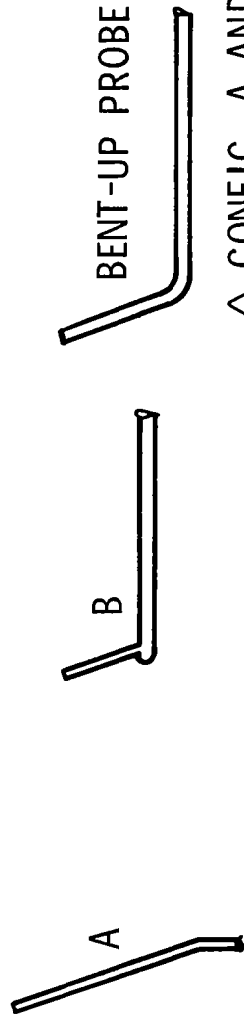


FIGURE 10

COMPARISON OF CONFIGURATIONS



- △ CONFIG. A AND B (REF. 1)
- IRVING (REF. 12)
- BENT-UP PROBE, CONFIG. 8
- BENT-UP PROBE, CONFIG. 11

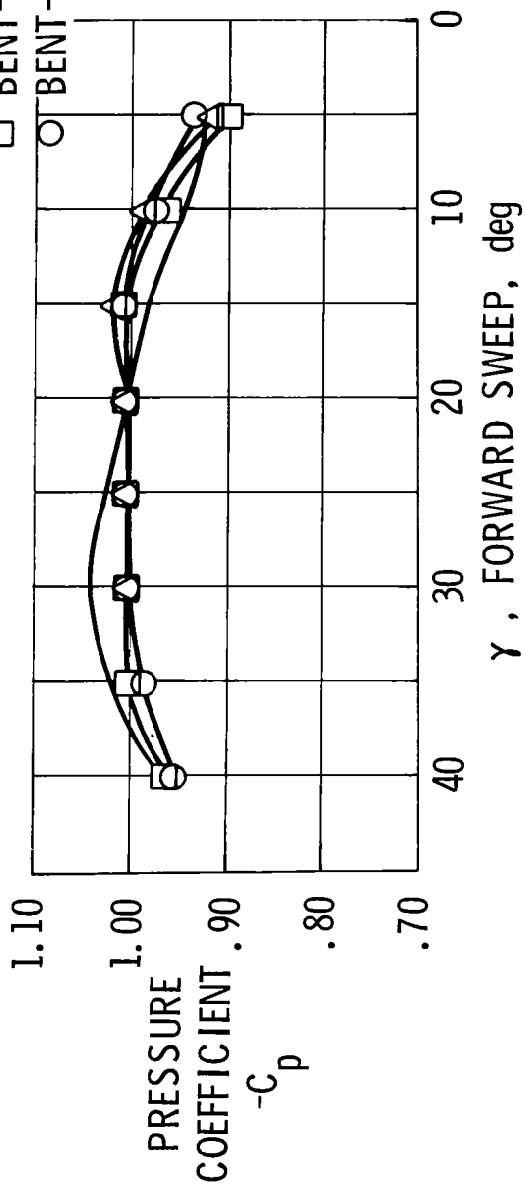


FIGURE 11

RESTRICTOR-CAPACITOR RELATIONSHIPS FOR TWO TIME CONSTANTS

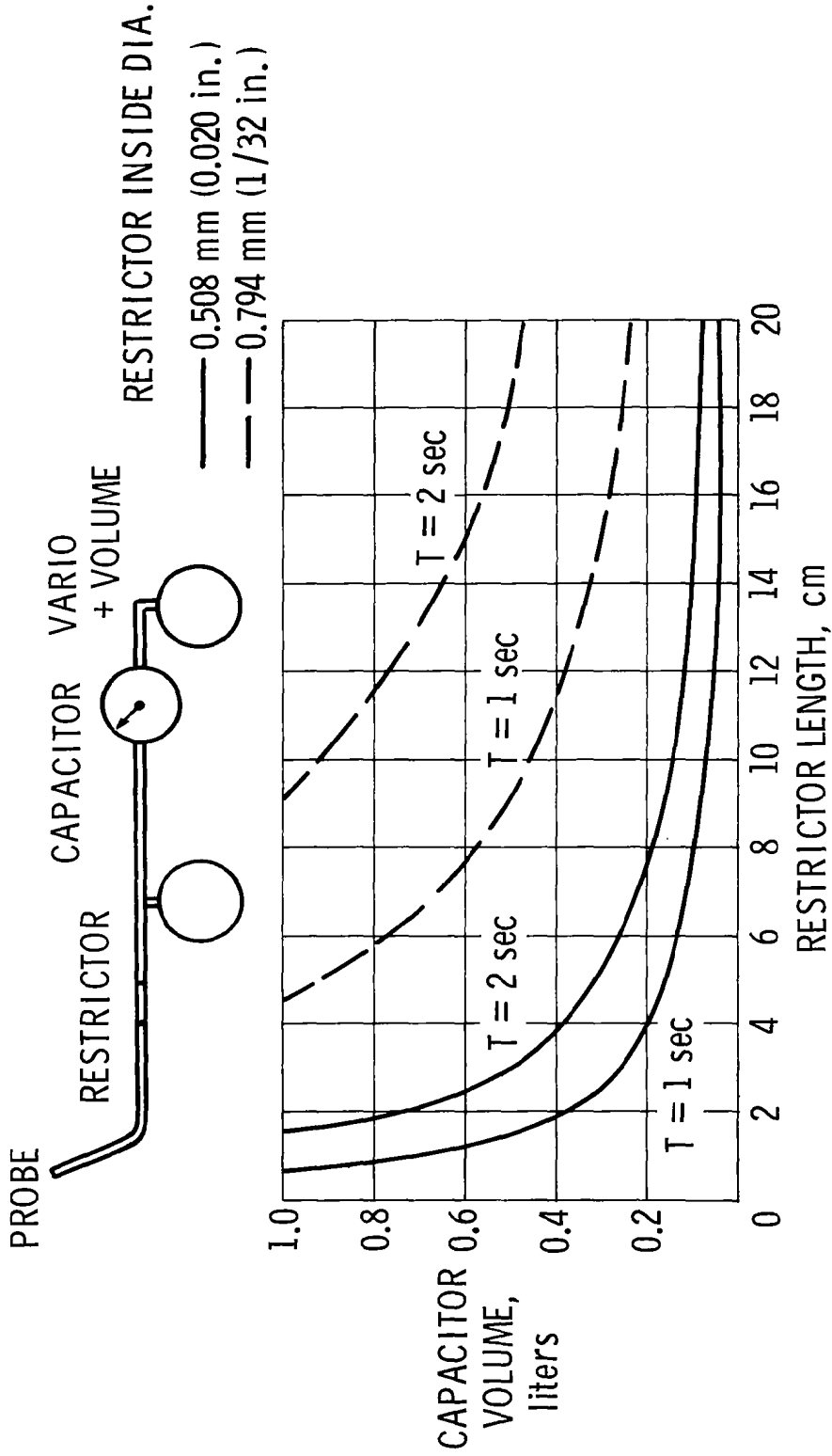


FIGURE I2